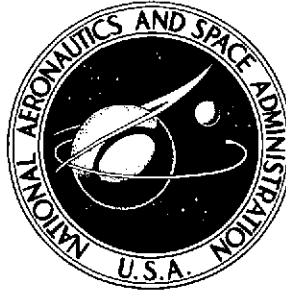


2m4

NASA TECHNICAL NOTE



NASA TN D-7514

NASA TN D-7514

(NASA-TN-D-7514)	BEHAVIOR OF HYDROGEN IN	N75-14187
	ALPHA-IRON AT LOWER TEMPERATURES (NASA)	
<del>29</del> p HC \$3 00 =	CSCL 11F	
30		Unclas
		H1/17 25276



# BEHAVIOR OF HYDROGEN IN $\alpha$ -IRON AT LOWER TEMPERATURES

*by Victor G. Weizer*  
*Lewis Research Center*  
*Cleveland, Ohio 44135*

1. Report No. NASA TN D-7514	2. Government Accession No.	3. Recipient's Catalog No.	
4. Title and Subtitle BEHAVIOR OF HYDROGEN IN $\alpha$ -IRON AT LOWER TEMPERATURES		5. Report Date December 1973	6. Performing Organization Code
		8. Performing Organization Report No. E-7496	
7. Author(s) Victor G. Weizer		10. Work Unit No. 501-21	11. Contract or Grant No.
9. Performing Organization Name and Address Lewis Research Center National Aeronautics and Space Administration Cleveland, Ohio 44135		13. Type of Report and Period Covered Technical Note	
		14. Sponsoring Agency Code	
12. Sponsoring Agency Name and Address National Aeronautics and Space Administration Washington, D. C. 20546		15. Supplementary Notes	
16. Abstract Evidence is presented that the low temperature anomalies in the hydrogen occlusive behavior of $\alpha$ -iron can be explained by means of a molecular occlusion theory. This theory proposes that the stable state of the absorbed hydrogen changes from atomic at high temperatures to molecular as the temperature is lowered below a critical value. Theories proposing to explain the anomalous behavior as being due to the capture, at lower temperatures, of hydrogen in "traps" are shown to be unacceptable.			
17. Key Words (Suggested by Author(s)) Hydrogen diffusion    Hydrogen embrittlement Hydrogen solubility $\alpha$ -iron		18. Distribution Statement Unclassified - unlimited	
19. Security Classif. (of this report) Unclassified	20. Security Classif. (of this page) Unclassified	21. No. of Pages 28	22. Price* Domestic, \$3.00 Foreign, \$5.50

\* For sale by the National Technical Information Service, Springfield, Virginia 22151

;

# BEHAVIOR OF HYDROGEN IN $\alpha$ -IRON AT LOWER TEMPERATURES

by Victor G. Weizer

Lewis Research Center

## SUMMARY

Evidence is presented that the low temperature anomalies in the hydrogen occlusive behavior of  $\alpha$ -iron can be explained by means of a molecular occlusion theory. This theory proposes that the stable state of the absorbed hydrogen changes from atomic at high temperatures to molecular as the temperature is lowered below a critical value. Theories proposing to explain the anomalous behavior as being due to the capture, at lower temperatures, of hydrogen in "traps" are shown to be unacceptable.

## INTRODUCTION

It is well known that the mechanical properties of iron and ferritic steels are adversely affected by the presence of hydrogen (ref. 1). When hydrogen is allowed to permeate these metals, they become less ductile and prone to delayed brittle fracture. The temperature and strain rate dependence of these mechanical properties indicate that the hydrogen diffusivity and solubility kinetics are intimately involved in the mechanism responsible for the observed loss of ductility. It follows, then, that in order to understand and control hydrogen embrittlement in these metals it is first necessary to have an understanding of the diffusion and solution processes operating therein.

A review of the available literature concerning the diffusion and solution of hydrogen in iron and steel reveals a confused state of affairs. The primary problem stems from the fact that both the diffusivity data and the solubility data exhibit large anomalies in the temperature range where hydrogen embrittlement is most severe. The following section of this report describes these anomalies and the theories put forth thus far to account for them. The succeeding section attempts to show that present views on the cause of the anomalous behavior which are based on the assumption of the existence of traps are untenable. A hypothesis is then advanced which suggests that the anomalous behavior is a manifestation of the fact that at low temperatures hydrogen in the iron lattice exists in the molecular state, while at high temperatures the atomic state is stable.

The symbols used in this report are defined in appendix A.

## EXPERIMENTAL AND THEORETICAL BACKGROUND

This section presents background data concerning the solubility and diffusivity of hydrogen in  $\alpha$ -iron and the explanations advanced in the literature to account for the observed facts. Let us look first at the diffusivity data.

The diffusion isobar shown in figure 1 is taken from reference 2. This curve illustrates the general features found in the literature: a linear high-temperature region, a break at some intermediate temperature, and a low-temperature region of higher slope. The data above the break are generally accepted as being the result of atomic diffusion of hydrogen in the iron lattice (ref. 3). The anomalous behavior in the low-temperature region remains unexplained in detail, although a number of suggestions have been made as to the origin of this effect. The activation energies associated with these two processes are measured to be about 10.5 and 33.5 kilojoules per mole (2.5 and 8 kcal/mole), respectively. The temperature at the discontinuity seems to be a weak function of the purity and the hydrogen content of the iron lattice.

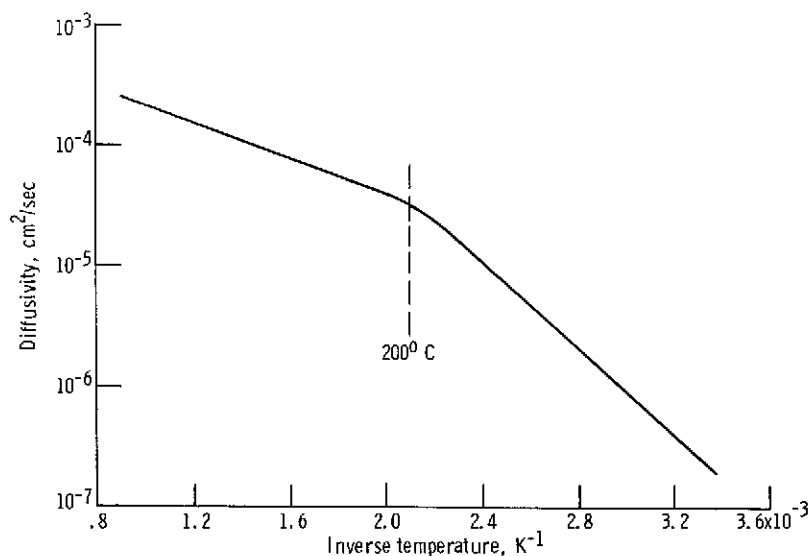


Figure 1. - Diffusion isobar for hydrogen in  $\alpha$ -iron. (Data from ref. 2.)

The solubility isobar in figure 2 is from reference 4, and here again a low-temperature anomaly is observed. From the slope of the well-behaved high-temperature region, the heat of solution is found to be about 25.1 kilojoules per mole (6 kcal/mole). For the low-temperature region, a value of about 4.19 kilojoules per mole (1 kcal/mole) is indicated. Whenever this discontinuity is observed, it always seems to occur at the same temperature (i.e.,  $400^\circ\text{C}$ ).

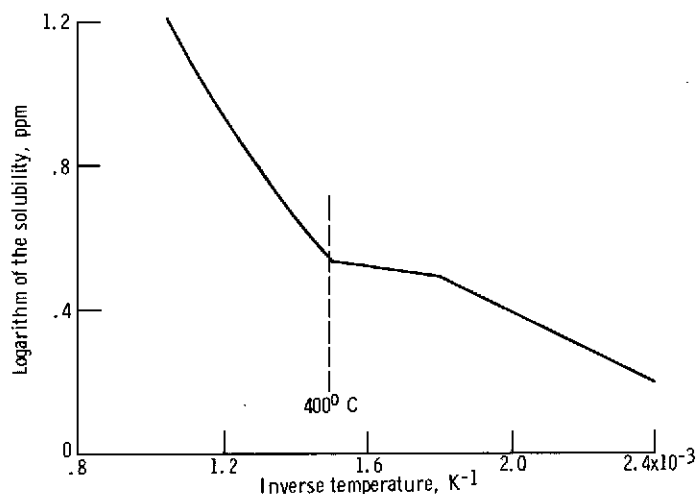


Figure 2. - Solubility isobar for hydrogen in  $\alpha$ -iron. (Data from ref. 4.)

The theories put forth to explain these data can be divided into three categories:

(1) Those based upon the assumption that at low temperatures surface processes are rate controlling, (2) those which postulate the existence of traps which alter the diffusion and solution kinetics, and (3) those which espouse a change with temperature of the state of aggregation of the hydrogen in the lattice.

The boundary-limited mechanisms have been shown to be untenable (ref. 5) and will not be discussed further.

A great majority of the investigators in the field subscribe to theories whereby, at low temperatures, hydrogen is held in "traps" from which it must be thermally activated before it can diffuse further (ref. 3). The depth of the potential wells associated with these traps is reasoned to be the difference between the activation energy for normal lattice diffusion, 12.6 kilojoules per mole (3 kcal/mole), and that for the anomalous low-temperature diffusion, 33.5 kilojoules per mole (8 kcal/mole), that is, about 21.0 kilojoules per mole (5 kcal/mole).

One of the main difficulties with this mechanism is that of identifying the traps. Suggested traps include dislocations (ref. 6), interstitials (refs. 7 and 8), cracks or voids (ref. 9), subgrain boundaries (ref. 10), rifts (ref. 11), etc. A potential diagram (from ref. 12) showing the energetic relations applicable to this model is presented in figure 3. It should be noted that the trapping model requires a greater solubility in the anomalous region than that expected from extrapolation from high temperatures. Consequently, a lower heat of solution is required in the low-temperature region (ref. 12). The trapping model also assumes that the trap concentration is much larger than the hydrogen concentration.

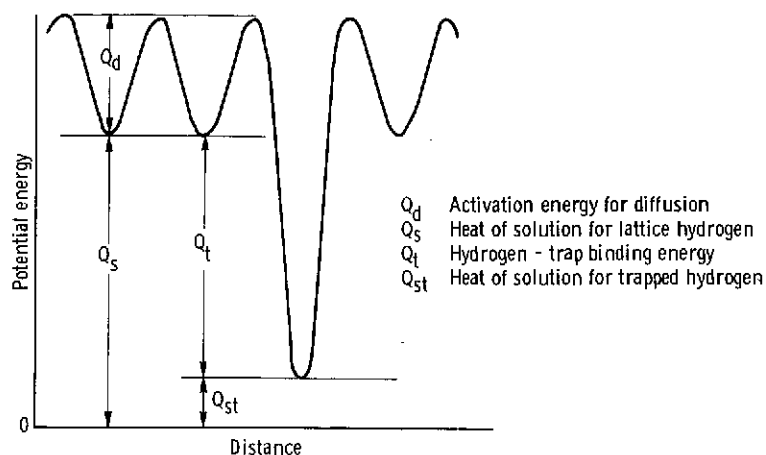


Figure 3. - Potential-energy diagram for trapping model.

A third mechanism is that advanced by Ham and Rast in 1938 (ref. 13) in an attempt to explain the low-temperature anomalies in their measured permeation rate data. They suggested that the "state of aggregation" of the hydrogen in the lattice changes at low temperatures as a result of a magnetic transformation that occurs in cementite. Ham and Rast do not elaborate any further on their model.

In the next section, after a critical examination of the data in the literature, an extension of Ham and Rast's suggestion of a "change in the state of aggregation" will be presented. Specifically, evidence will be given that, at lower temperatures, hydrogen exists in a molecular state in the iron lattice. This would suggest, then, that the break in the diffusion isobar is caused by the association of pairs of hydrogen atoms as the temperature is lowered below about 200<sup>0</sup> C. However, while it seems clear from the arguments that follow that this molecular occlusion theory is valid, an explanation of the underlying causes of the low-temperature association must await further study.

### CASE FOR MOLECULAR OCCLUSION

The purpose of this section is to show that (1) the 400<sup>0</sup>-C solubility anomaly measured by various investigators is independent of the 200<sup>0</sup>-C diffusion anomaly and can, in fact, be completely eliminated by improving the purity of the iron, (2) there is a solubility anomaly associated with the diffusion anomaly which, while inconsistent with a trapping model, is explained by the molecular occlusion model, (3) there is evidence from the pressure dependence of the solubility that molecular hydrogen does enter and diffuse in iron at low temperatures, and (4) the proposed molecular occlusion model seems to tie together in a consistent manner many of the accumulated facts concerning the behavior of hydrogen in iron.

## General Argument

As mentioned previously, the hypotheses that attribute the low-temperature diffusion anomaly to the delay of the diffusing hydrogen in traps require that the low-temperature solubility (in the trapping region) be higher than expected from extrapolation of the normal high-temperature solubility data. Associated with this increased solubility, of course, would be a reduced heat of solution.

The main experimental evidence for this increase in solubility is the data of reference 4, where a low-temperature ( $T < 400^{\circ}\text{C}$ ) heat of solution of about 4.19 kilojoules per mole (1 kcal/mole) is indicated (fig. 2).

Upon close consideration of the data concerning the  $400^{\circ}\text{C}$  solubility anomaly, one can show that it can be completely eliminated without affecting the diffusivity anomaly. Let us start by considering the work of Keeler and Davis (ref. 14) and that of Evans and Rollason (ref. 15).

Keeler and Davis measured the effect of cold work on both the hydrogen occlusive capacity and the density of iron and varying carbon content. Their measurements of the effect of cold work on the density of relatively pure iron (0.006-percent carbon) and iron of significant carbon content are shown in figure 4. One can see that, for carbon-free iron, the density is not affected even though the specimens are severely cold worked. The carbon steels, on the other hand, show a reduction in density upon being cold worked. Keeler and Davis interpret the density decrease as being due to the presence of cracks and voids produced during mechanical deformation in the carbon-containing specimens.

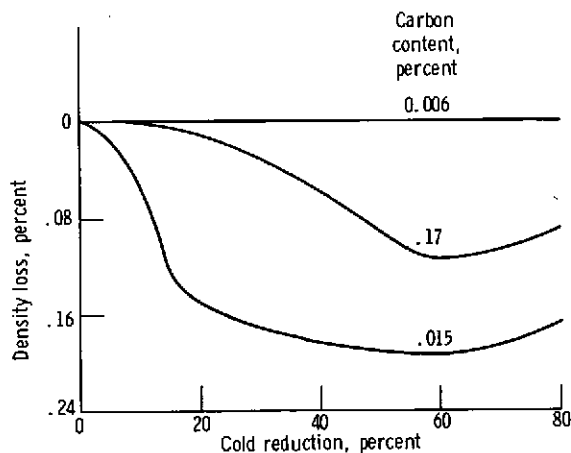


Figure 4. - Variation of density with cold work for iron containing various amounts of carbon. (Data from ref. 14.)

If we look now at the effect of cold work on hydrogen solubility in these metals (fig. 5), we see that while the carbon-containing specimens show a large increase in the solubility below 400° C, the carbon-free (0.006-percent carbon) material under the same deformation conditions is well behaved all the way down to 250° C. The solubility data of Hill and Johnson (ref. 9) for varying amounts of cold work are also shown in figure 5. It appears that for carbon-free iron there is no anomalous behavior below 400° C, but for carbon-containing specimens the degree of anomalous occlusion is a function of the amount of plastic deformation. The obvious conclusion, as stated by

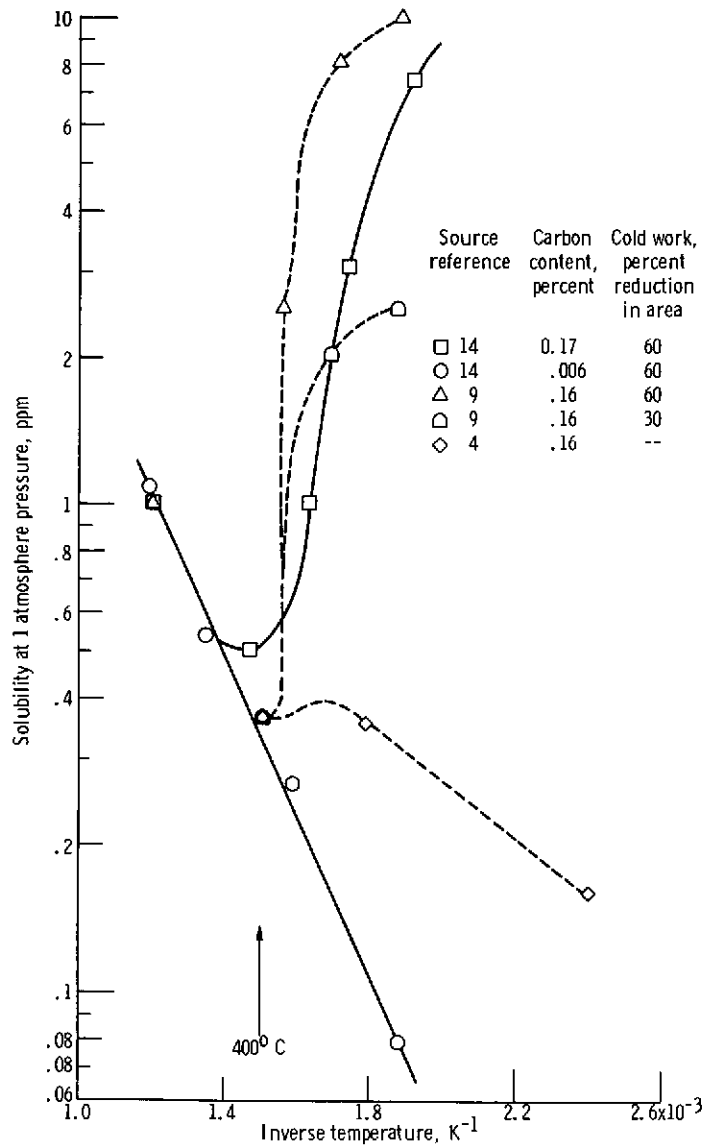


Figure 5. - Effect of cold work on solubility of hydrogen in iron containing various amounts of carbon.

Keeler and Davis, is that the anomalous occlusion takes place in the cracks and voids produced when carbon-containing material is cold worked.

A demonstration of the fact that the 400<sup>o</sup>-C solubility anomaly can be removed, however, does not establish the fact that this process is independent of the diffusion anomaly. To do this, let us consider the work of Evans and Rollason (ref. 15), who performed essentially the same purity, density, cold-work study on the diffusion characteristics of iron. Their results on the effect of cold reduction on the density and the room-temperature diffusion coefficient are shown in figures 6 and 7 for specimens of different carbon content. Here again, removal of carbon makes the density independent of cold work. However, while the diffusion coefficient of the pure sample is, in a manner similar to the solubility, not affected by the mechanical working, it remains anomalously low.

Thus, although the 400<sup>o</sup>-C solubility anomaly can be eliminated by removing carbon impurities from the iron, the diffusivity anomaly cannot be so removed. These two anomalies, therefore, must be manifestations of two independent phenomena.

Having shown now that the 400<sup>o</sup>-C solubility anomaly is independent of the diffusion anomaly, one wonders whether there is another solubility anomaly connected with the diffusion anomaly and, if so, whether it is compatible with a trapping hypothesis.

It has been pointed out that changes in either the solubility or the diffusivity due to trapping effects cannot be detected in steady-state permeation measurements. Thus, the permeation isobars would not give any indication of a change in slope, even if trapping phenomena were occurring at low temperatures.

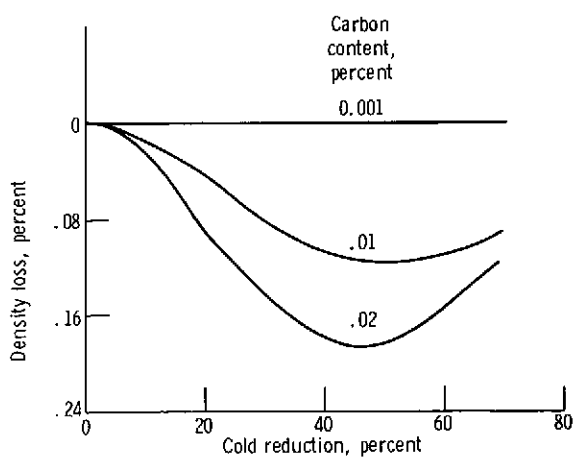


Figure 6. - Variation of density with cold work for iron containing various amounts of carbon. (Data from ref. 15.)

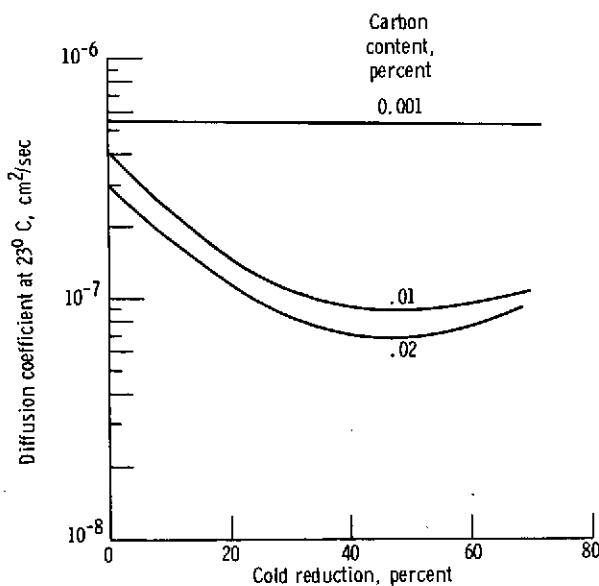


Figure 7. - Effect of cold work on diffusion coefficient of hydrogen in iron containing various amounts of carbon. (Data from ref. 15.)

Inspection of the permeation isobars of Ham and Rast (ref. 13) and Chang and Bennett (ref. 16), however, reveals a break to higher slope as the temperature is lowered below a critical value. This break can only be interpreted as evidence of an increase in the lattice diffusion activation energy, the lattice heat of solution, or both. This statement is predicated, of course, on the condition that surface processes are not limiting at lower temperatures. Justification for this assumption is presented in appendix B.

Further, we can obtain a value for the heat of solution,  $Q_s$ , in the anomalous region from the activation energy for permeation,  $Q_p$ , and the anomalous diffusion activation energy,  $Q_d$ . Values of  $Q_p$  and  $Q_d$  are given in table I along with the calculated heats of solution for both the high-temperature region and the anomalous low-temperature region, where the relation

$$Q_p = Q_d + Q_s$$

was used. As can be seen, there is an anomaly in the solubility at low temperatures. Furthermore, the anomalous heat is larger than the normal high-temperature heat. This observation is interesting in that the trapping models predict a lower heat of solution in this temperature region.

These deductions cast serious doubt on the use of a trapping hypothesis to explain the anomalous diffusion behavior, since the permeation isobar should not show a break if trapping were taking place. Accordingly, the trapping hypotheses will henceforth be considered untenable, and an effort will be made to determine the consistency with which the molecular occlusion model explains the observed facts.

Let us postulate, then, a model whereby, above a critical temperature, hydrogen exists in atomic form in the lattice, and, as the temperature is lowered below that critical temperature, the atoms for some reason associate into molecules, in which state they migrate through the lattice. Further, let us assume that because of its small size, the molecule resides in a single interstice. Evidence to support such a postulate is derived from the observed pressure dependence of the solubility.

The relation between the solubility  $S$  in a solid medium and the pressure  $P$  of the surrounding as is given by

$$S = KP^n \exp - Q_s/kT$$

where  $Q_s$  is the heat of solution,  $K$  and  $n$  are constants, and  $kT$  has its usual meaning. From the slope of a logarithmic plot of the solubility against the pressure, we can obtain information concerning the mode of existence of the hydrogen in the iron lattice. If  $n$  (the slope) is unity, then the hydrogen is being occluded as molecules, and if  $n$  is

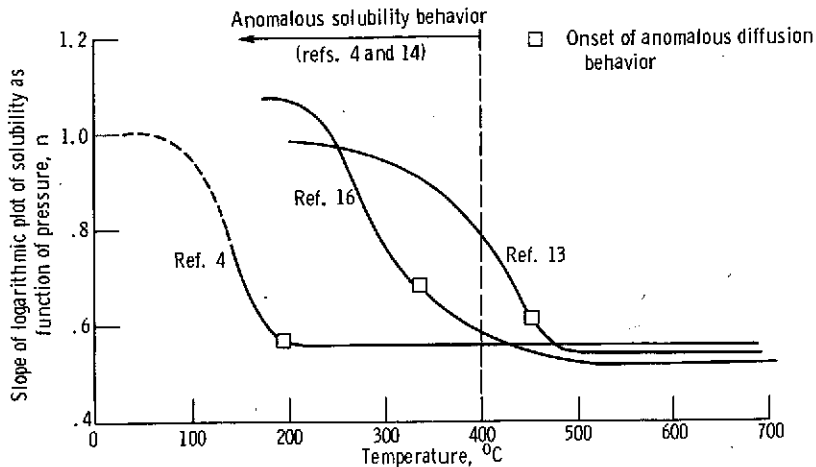


Figure 8. - Effect of temperature on pressure dependence of solubility of hydrogen in iron.

0.5, atomic hydrogen is being occluded.

In figure 8 are plotted the values of  $n$  measured by several investigators (refs. 4, 13, and 16) as a function of temperature. This pressure dependence indicates a change from atomic occlusion at high temperatures to molecular occlusion at low temperatures. Although attempts have been made to explain deviations from the square-root dependence as being due to electronic interactions (ref. 17), the fact that the change in the measured pressure dependence is not merely a deviation but a definite switch from a square-root dependence to a linear dependence leads one to accept the occlusive mode change explanation.

In analogy to figure 3 for the trapping model, we can construct a potential diagram, shown in figure 9, for the present model. Figure 9(a) shows the situation envisioned for high temperatures. Here the molecular heat of solution is large, the energetically favorable state being atomic. However, when the temperature is lowered below the critical value ( $T \approx 200^{\circ}\text{C}$ ), the molecular heat suddenly drops, and the atomic heat rises, so that the molecular state becomes stable (fig. 9(b)). These abrupt changes in the heats of solution are necessary to assure that only atomic occlusion occurs above the critical temperature and only molecular occlusion occurs below. The reference potential for figure 9 is that for a hydrogen molecule at rest in the gas phase a large distance from the iron surface. Also, in figure 9 we must use the energy needed to add 2 moles of hydrogen atoms to the crystal for the case of atomic occlusion in order to be able to make an energy comparison between this case and molecular occlusion. Speculation as to the value of the binding energy  $Q_b$  will be presented later in this report.

Since it would bolster confidence in the present model if we could show that it would be theoretically feasible to expect the diffusion activation energy to increase by a factor

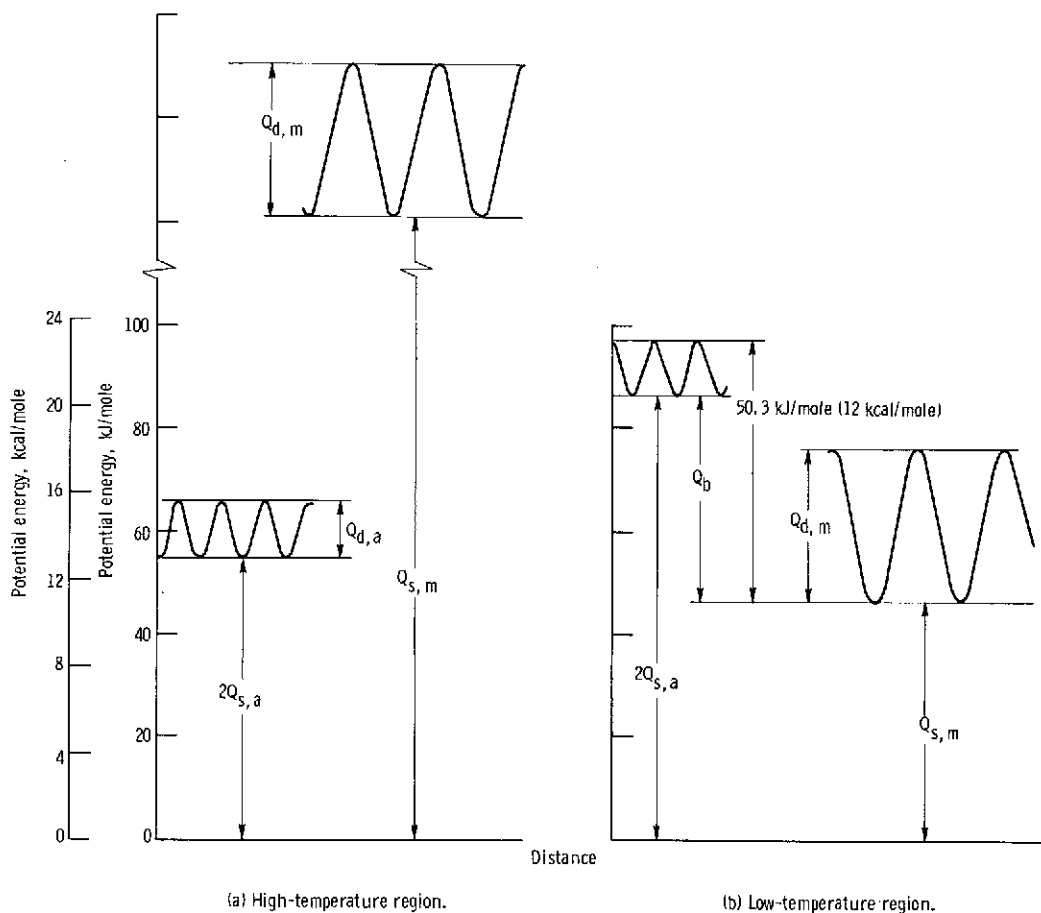


Figure 9. - Potential-energy diagrams for high- and low-temperature regions for molecular-occlusion model.

of 2 or 3 when the proposed atomic-to-molecular conversion takes place, it seemed worthwhile to perform a calculation similar to that of reference 18 on the iron-carbon system with the use of computer simulation techniques.

While the details of the calculations are given in appendix C, the basic approach was as follows: An iron-hydrogen potential function was constructed by requiring the model to reproduce the activation energy for atomic diffusion, 12.6 kilojoules per mole (3 kcal/mole), when the radius of the diffusing species is that for atomic hydrogen,  $5 \times 10^{-9}$  centimeter (0.5 Å). This potential function, along with a previously determined iron-iron potential function (ref. 19), was used to calculate the activation energy for interstitial diffusion as a function of the size of the diffusing species. The results, shown in figure 10, should give an indication of the relative ease of diffusion of hydrogen in the atomic and in the molecular state. It should be mentioned that in these calculations the hydrogen molecule is assumed to reside in a single interstice (which is reasonable because of its small dimension) and to possess spherical symmetry.

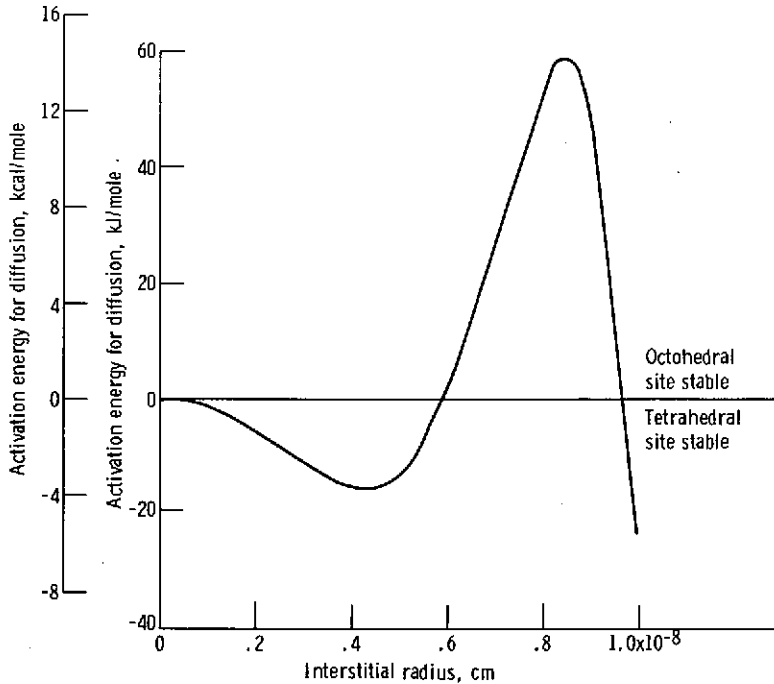


Figure 10. - Calculated activation energy for diffusion of hydrogen in  $\alpha$ -iron as a function of the radius of the diffusing species.

The behavior indicated in figure 10 is as follows: For small radii (atomic occlusion), the stable position is the tetrahedral site, and the activation energy (forced by the input to the calculations) is of the order of 12.6 kilojoules per mole (3 kcal/mole). For larger radii, the stable position shifts from the tetrahedral to the octohedral site, and the activation energy for diffusion increases to 3 or 4 times that for atomic diffusion. Specifically, if we assume a molecular radius of  $7.5 \times 10^{-9}$  centimeter ( $0.75 \text{ \AA}$ ), half of twice the internuclear distance of the hydrogen molecule (ref. 20), the calculated activation energy is 33.5 kilojoules per mole (8 kcal/mole), which is in agreement with the measured value.

The feasibility of the molecular occlusion concept, then, is enhanced in that a simple model can be constructed that describes very closely the physical phenomena that are to be accounted for.

### Critical Temperature

We have seen that the pressure dependence of the permeation rate changed from a square-root dependence to a linear dependence as the temperature was lowered below a critical value. Let us now use this deviation to obtain a plot of the variation of the criti-

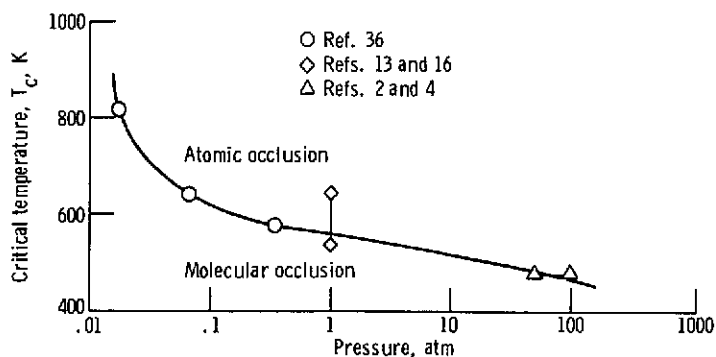


Figure 11. - Variation of critical temperature for conversion from atomic to molecular occlusion as a function of hydrogen pressure.

cal temperature with pressure as in figure 11. This plot indicates that even at relatively high temperatures, hydrogen is occluded in the molecular state if the pressure is sufficiently low.

Conversely, if the pressure or its equivalent is high enough, atomic occlusion can be induced down to room temperature and below. This behavior can be observed in specimens electrolytically charged with hydrogen. It has been reported by Smialowski (ref. 21) that for low current densities, the permeation rate of hydrogen through iron is proportional to the current density, whereas at high current densities, a square-root relation holds. (It is assumed here that the current density used in cathodic charging techniques is the equivalent of the pressure in gaseous charging methods (ref. 22).) Thus, by increasing the current density, or the pressure, to high values, one can force atomic occlusion at room temperature. Furthermore, as will be shown in the next section, internal friction measurements indicate that the conversion temperature can be depressed far below room temperature if the current densities used are sufficiently high.

The most obvious effect of increasing the pressure is the increase in hydrogen concentration in the specimen. If the concentration were the deciding factor, then, for any given temperature, there would be a critical value of the hydrogen concentration above which occlusion is atomic and below which molecular hydrogen is more stable. This reasoning seems to be verified by the observations made on plated internal friction specimens discussed in the next section, although the possibility that either the rate of entry or the concentration gradient may play a role cannot be ruled out.

### Internal Friction

Since anelastic damping methods have been used to observe the diffusion of interstitial solutes in metallic lattices, and in particular, the diffusion of hydrogen in iron,

the question arises as to whether the postulated molecular diffusion of hydrogen in iron might be observed by this technique. The question is doubly interesting since there exists a damping peak for hydrogenated iron which has an activation energy associated with it of approximately 33.5 kilojoules per mole (8 kcal/mole) (refs. 6 and 23), about the same as that for the low-temperature diffusion anomaly. The existing opinion in the literature, however, is that this anelastic phenomenon is due to the coupled motion of hydrogen interstitials and dislocations created by plastic deformation. Furthermore, the arguments presented are well documented and seem indisputable (ref. 23). It would seem, then, that if molecular diffusion is detectable by internal friction methods, evidence for it must be sought elsewhere in the damping spectrum. Unfortunately, the iron-hydrogen spectrum does not show evidence of another peak with characteristics that would be expected from molecular diffusion.

However, if one considers the internal friction data in light of the above-mentioned concentration effect, one sees that these investigators very possibly induced the atomic state in their specimens by severe charging methods, probably used in an attempt to ensure a sufficiently large damping response. In other words, because of the cathodic charging techniques used (refs. 6 and 23 to 26), the hydrogen concentration in the samples was very possibly high enough that occlusion in the atomic state was preferred. We would not, therefore, expect to see a molecular Snoek peak under these conditions.

It follows, then, that in order to observe the molecular peak, the amount of hydrogen in the lattice would have to be reduced, perhaps by aging at elevated temperatures. Weiner and Gensamer (ref. 24) performed such an aging experiment, and their results did, indeed, show a previously undetectable damping peak. Their aging curves are reproduced in figure 12. The figure indicates the existence of not one but two peaks: one at about 100 K, and one about 15 K higher.

The results for the non-cold-worked specimen, figure 12(a), show that after charging, there is little evidence of either peak. After the sample has been allowed to degas at 300 K for several days, however, the lower-temperature peak appears and grows. Further aging (degassing) of the sample causes the lower-temperature peak to fade away. The higher-temperature peak in figure 12(a) does not seem to be affected by the aging process. The results for the cold-worked sample, figure 12(b), show that the effect of plastic deformation is to increase the magnitude of the higher-temperature peak, while the lower-temperature peak remains unchanged. The obvious conclusion, then, is that the higher-temperature peak is the "cold-work peak" which has been studied rather extensively (ref. 23), and that the lower-temperature peak, which is not affected by cold work and which only appears after much of the hydrogen has left the sample, is the molecular Snoek peak.

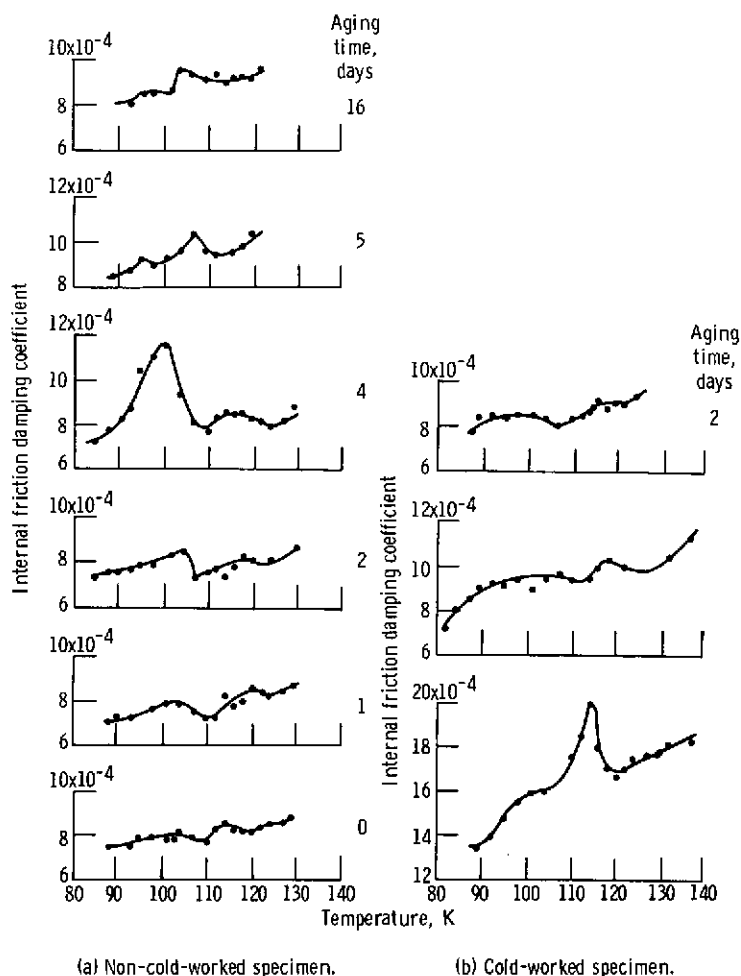


Figure 12. - Effect of aging (degassing) on dual internal-friction peaks of hydrogen-charged iron. (Data from ref. 24.)

A pair of peaks in this temperature range, separated by about  $15^{\circ}$ , and attributed to the presence of hydrogen, have also been observed by Heller (ref. 25, fig. 7) and by Maringer et al. (ref. 26, fig. 30). For some reason, the temperatures associated with these peaks vary from investigator to investigator in such an erratic manner that the energies corresponding to the peaks cannot be obtained from the peak shift with frequency if data from different sources are used. In view of this, only those activation energies derived from measurements performed on identical specimens can be trusted. For the lower-temperature peak this has not yet been done.

It is also of interest to consider the damping measurements of Lord (ref. 27). He observed a narrow peak at 120 K which appeared after mild pressure charging but which did not appear after heavy cathodic charging. Although Lord did not measure the activation energy associated with the peak, he attempted to identify it with the atomic hydrogen Snoek peak. The evidence that the peak appears only at reduced hydrogen concen-

trations suggests that what Lord observed was, rather, the molecular Snoek peak. An experimental determination of the characteristics of the peak in question must be made, however, before we can positively identify it as the molecular Snoek peak.

It should be noted that the growth of the molecular peak is not seen in the aging experiments of either Gibala (ref. 23) or Sturges and Miodownik (ref. 6). The maximum aging time in these two investigations, however, was of the order of hours, whereas the time required to bring out the peak observed in reference 24 was of the order of days. Furthermore, the specimens of both references 6 and 23 were severely cold worked, and cold work seems to inhibit the growth of the lower-temperature peak, as was indicated by figure 12(b).

### Binding Energy

As stated previously, the magnitude of the binding energy  $Q_b$  (fig. 9) is not known. There is, however, an activated process that takes place in the low-temperature region - the 50.3-kilojoule-per-mole (12-kcal/mole) diffusion process reported in references 28,

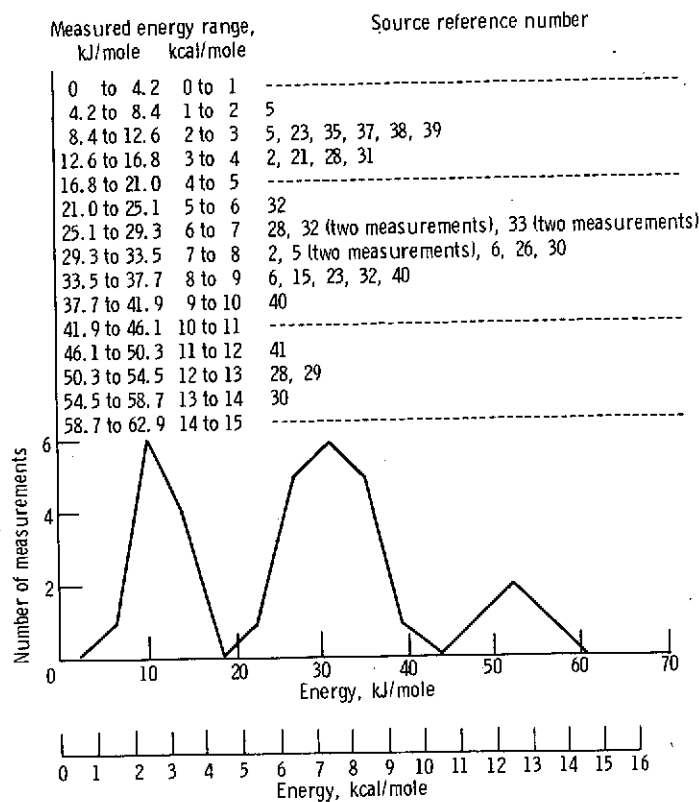


Figure 13. - Distribution of measured activation energies for diffusion of hydrogen in iron.

29, and 30 - which has not yet been explained. This peak is evident in figure 13, where the distribution of measured activation energies is plotted. I will now speculate and suggest a possible relation between the 50.3 -kilojoule-per-mole (12-kcal/mole) process and  $Q_b$ .

Let us assume a diffusion specimen that is composed mainly of regions of molecular occlusion, but contains, in addition, some noninterconnecting regions where, for some reason, molecular occlusion is forbidden. There are two diffusion paths in such a material: (1) diffusion in molecular regions only, and (2) diffusion through alternate regions of atomic and molecular occlusion. The situation is illustrated schematically in figure 14.

When a diffusing hydrogen molecule (path 2) comes upon a region of atomic occlusion, it must receive activation of the order of, let us assume, 50.3 kilojoules per mole (12 kcal/mole) in order to enter the region. Once activated into the atomic region, however, the hydrogen atoms would be able to diffuse very rapidly because of the low activation energy, 10.5 kilojoules per mole (2.5 kcal/mole), in that region. If diffusion through the atomic regions were fast enough, and the number and size of the regions large enough, diffusion along path 2 (with a large activation energy) might be expected

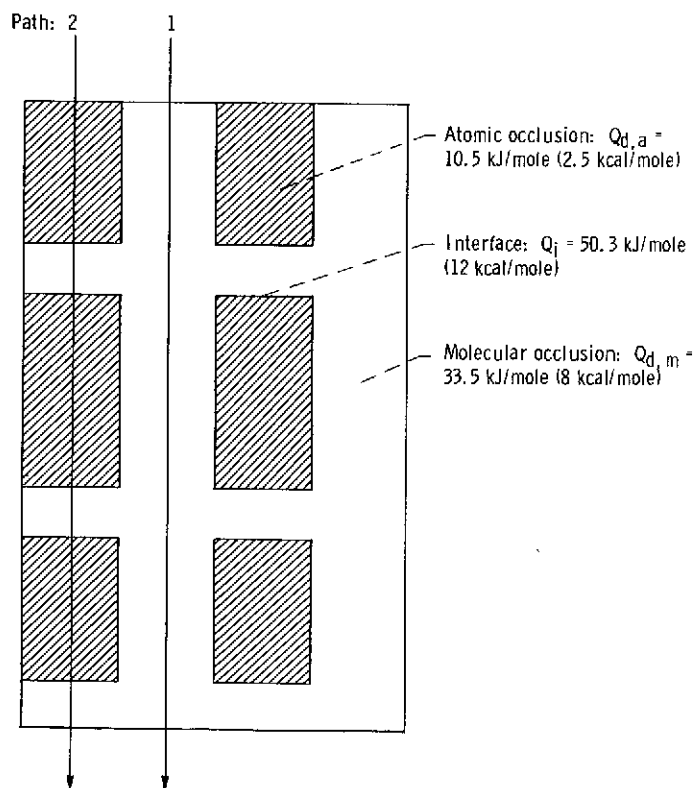


Figure 14. - Schematic diagram of diffusion paths in hypothetical diffusion specimen.

to be faster at high temperatures than diffusion along path 1. The diffusion isobar would, therefore, be expected to break to a higher slope as the temperature is increased. Further, the rapid diffusion through the regions of atomic occlusion would be reflected in a large value of  $D_0$ , the diffusion preexponential, for the 50.3-kilojoule-per-mole (12-kcal/mole) process.

Both the conversion from molecular to bi-phase diffusion as the temperature is raised and the large value of  $D_0$  are exhibited in the experimental measurement of reference 30. The isobars from reference 30 for both hydrogen and deuterium are shown in figure 15. At low temperatures, the diffusion is molecular. As the temperature is

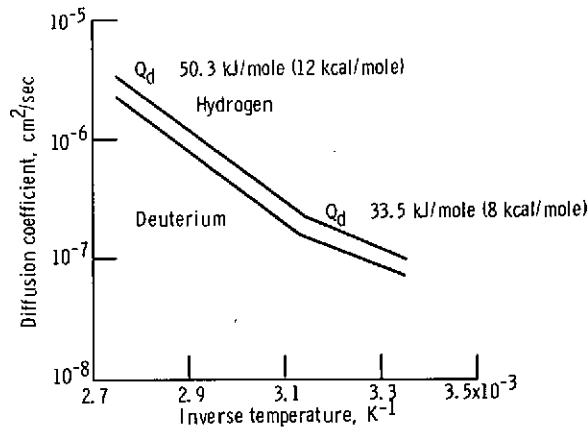


Figure 15. - Low-temperature diffusion isobars for both hydrogen and deuterium, showing onset of the 50.3-kilojoule-per-mole (12-kcal/mole) process. (Data from ref. 30.)

raised, the 50.3-kilojoule-per-mole (12-kcal/mole) process dominates. Also, the value of  $D_0$  in these measurements is greater than that for normal diffusion by a factor of  $10^4$ . Assuming the validity of the above reasoning,  $Q_b = 38.6$  kilojoules per mole (9.5 kcal/mole).

Since this phenomenon was observed in material that had been cold worked, it is suggested that perhaps the plastic deformation is somehow responsible for the production of the postulated regions of forbidden molecular occlusion.

Experimental measurement of the heat of solution associated with the 50.3-kilojoule-per-mole (12-kcal/mole) process would provide a test of these suggestions.

## SUMMARY OF RESULTS

The results of this investigation into the nature of the anomalous behavior of the solubility and the diffusivity in the iron-hydrogen system can be summarized as follows:

1. The 400<sup>o</sup> -C solubility anomaly, which is due to the extra lattice occlusion of hydrogen in voids and cracks formed during plastic deformation, was shown to be completely independent of the low-temperature diffusivity anomaly.

2. The existence of a previously unrecognized anomaly in the solubility kinetics that is associated with the diffusivity anomaly was demonstrated. The heat of solution was determined to be 46.1 joules per mole (11 kcal/mole).

3. The use of a trapping hypothesis to explain these anomalous effects was shown to be unacceptable.

4. A molecular occlusion hypothesis was proposed that accounts for the observed anomalous behavior.

5. The molecular occlusion theory was shown to tie together in a consistent manner many of the confusing and hard-to-account-for data encountered in the study of the iron-hydrogen system.

6. The investigation indicated the need for further experimental work. In particular, the characteristics of the 100 K internal-friction peak, the solution properties of the 50.3-kilojoule-per-mole (12-kcal/mole) process, and the effect of cold work on the process need to be determined.

Lewis Research Center

National Aeronautics and Space Administration

Cleveland, Ohio, August 15, 1973,

501-21.

## APPENDIX A

### SYMBOLS

D	energy of a pair of atoms at equilibrium separation
$D_0$	diffusion preexponential
K	constant used in the solubility equation
k	Boltzman's constant
n	constant (exponent) used in the solubility equation (slope of a logarithmic plot of solubility as a function of pressure)
P	pressure
$Q_b$	binding energy of hydrogen molecule in the iron lattice
$Q_d$	activation energy for diffusion
$Q_{d,a}$	activation energy for atomic diffusion
$Q_{d,m}$	activation energy for molecular diffusion
$Q_i$	energy required for thermal activation from region of molecular occlusion to region of atomic occlusion
$Q_p$	activation energy for permeation
$Q_{ST}$	heat of solution for trapped hydrogen
$Q_s$	heat of solution
$Q_{s,a}$	heat of solution - atomic occlusion
$Q_{s,m}$	heat of solution - molecular occlusion
$Q_T$	hydrogen-trap binding energy
$r_{ij}$	separation between a pair of atoms, i and j
$r_0$	equilibrium separation of a pair of atoms
S	solubility
T	temperature
$T_c$	critical temperature
$\alpha$	constant that influences the detailed shape of the Morse potential function
$\varphi_{ij}$	energy of a pair of atoms, i and j

## APPENDIX B

### SURFACE RATE-CONTROLLING PROCESSES

An important point in this discussion is whether the breaks in the isobars of Ham and Rast (ref. 13) and Chang and Bennett (ref. 16) are due to bulk effects or to surface effects.

Some investigators have assumed that surface effects are rate controlling at lower temperatures (ref. 17). There is, however, no evidence to support this assumption. In fact, all attempts to show that surface processes are limiting in the iron-hydrogen system at low temperatures have produced negative results. We can cite here the diffusion work of references 2, 28, 29, and 31, and the permeation experiments of references 32 and 33.

The conversion of the pressure dependence of the solubility from a square-root dependence at high temperatures to a linear dependence at low temperatures cannot be used as evidence of surface control at low temperatures because it has occurred also in investigations where bulk diffusion were shown to be the limiting process (refs. 2 and 4).

The presence of water or water vapor has been observed by a number of investigators to effect an increase in the rate of effusion of hydrogen from iron over the effusion rate into vacuum or other media (ref. 3). However, the fact that the diffusion coefficients measured by these investigators using a moisture-free atmosphere agree with the values measured by others where bulk processes were known to be rate controlling indi-

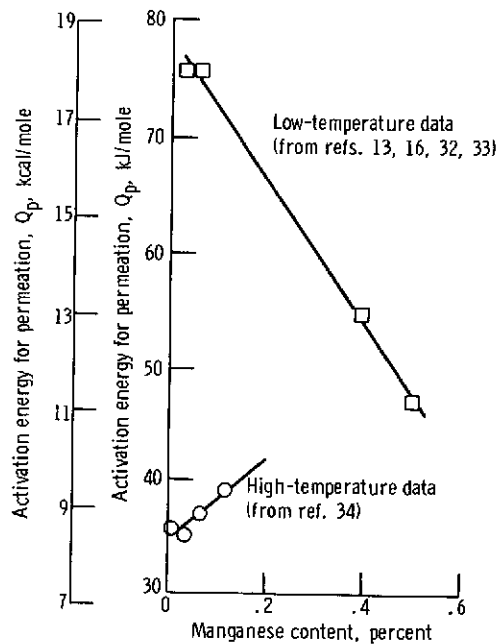


Figure 16. - Activation energy for hydrogen permeation in iron as a function of manganese content for both the high-temperature and the low-temperature regions.

cates that the effect of the water must be other than a surface rate limiting effect (ref. 3).

Gonzales (ref. 34) has analyzed the permeation-rate data in the literature and has concluded that impurities, notably manganese, have the effect of increasing the activation energy for permeation (fig. 16). He concludes that this is a surface effect, assuming the impurity content does not appreciably affect either the activation energy for diffusion or the heat of solution of hydrogen in iron. However, the data of Geller and Sun (ref. 35) show that the activation energy for diffusion is drastically affected by the presence of manganese and silicon impurities. It is highly probable, then, that the variation in the permeation energy reported in reference 34 is due to a variation in the activation energy for diffusion and not to surface effects.

Another point that should be discussed here is the fact that both Choi (ref. 32) and Eschbach, Gross, and Schulein (ref. 33) measured activation energies for permeation at low temperatures that do not agree with the values obtained by either Ham and Rast (ref. 13) or Chang and Bennett (ref. 16). Again, this discrepancy can be correlated with manganese impurities in the steel. A plot of the permeation activation energy in the low-temperature region as a function of manganese content is given in figure 16 where a linear relation is indicated. At low temperatures, the purer the iron, the higher the activation energy, which is contrary to the behavior in the high-temperature region.

It is interesting to note in figure 16 that the intersection of the high-temperature data with the low-temperature data occurs at a manganese content of about 4 percent, corresponding to an activation energy of about 54.5 kilojoules per mole (13 kcal/mole). At this manganese content, then, the slopes in both the high-temperature and low-temperature regions would be the same, and one would not expect a break in the permeation isobar. This is probably the case in the data of reference 33.

In summary, there is no evidence that surface processes control hydrogen permeation in iron at low temperatures. To the contrary, there is much data that shows that surface processes are not limiting in this system. Manganese and silicon affect the permeation activation energies. For pure iron, the value of the high-temperature permeation energy is about 35.2 kilojoules per mole (8.4 kcal/mole), and the low-temperature value is in the vicinity of 75.4 kilojoules per mole (18 kcal/mole).

## APPENDIX C

### COMPUTER SIMULATION CALCULATIONS OF DIFFUSION

#### ACTIVATION ENERGIES

To obtain a rough idea of how the behavior of atomic hydrogen in the iron lattice differs from that of molecular hydrogen, an attempt was made to calculate the migration and site energies for these two species with the use of computer simulation techniques similar to those used by Johnson, Dienes, and Damask (ref. 18) for the iron-carbon system.

A Morse type potential function was chosen because of its simplicity and because a reliable iron-iron potential function had already been constructed (ref. 19). The Morse potential function specifies the relation between the energy  $\varphi_{ij}$  of a pair of atoms,  $i$  and  $j$ , and their separation,  $r_{ij}$ . Thus,

$$\varphi_{ij} = D \left\{ \exp \left[ -2\alpha(r_{ij} - r_0) \right] - 2 \exp \left[ -\alpha(r_{ij} - r_0) \right] \right\}$$

where  $r_0$  is the equilibrium separation,  $D$  is the energy of the pair at equilibrium separation, and  $\alpha$  is a constant that influences the detailed shape of the function.

Because hydrogen occlusion in iron is an endothermic process, the hydrogen-iron binding energy,  $D$ , is small. In these calculations, therefore,  $D$  was arbitrarily set at 3.39 kilojoules per mole (0.035 eV), one-tenth the value determined in the iron-carbon calculations of reference 18. Although the attractive component of the potential was thus made quite small, the residual minimum served as a mathematical definition of equilibrium separation.

Because of the small internuclear distance of molecular hydrogen,  $7.4 \times 10^{-9}$  centimeter (0.74 Å), it seemed reasonable to assume that only one interstice is involved in the occlusion of a molecule. The model also assumes spherical symmetry for both the atomic and the molecular species.

The value of  $\alpha$  was chosen so that when  $r_0$  corresponded to the sum of the radius of the Morse iron atom,  $1.42 \times 10^{-8}$  centimeter (1.42 Å), and the radius of a hydrogen atom,  $5 \times 10^{-9}$  centimeter (0.5 Å), the calculations correctly reproduced the known value of the activation energy for atomic diffusion, 12.6 kilojoules per mole (3 kcal/mole). The value of  $r_0$  was then varied, and the migration energy was calculated as a function of the size of the diffusing species. It should be noted that this procedure assumes the molecular and atomic potential functions to differ only through the value of  $r_0$ .

The atoms involved in the calculation were the interstitial atom, its nearest neighbors, and the nearest neighbors to the nearest neighbors. Only the nearest neighbors to the interstitial atom were permitted to relax.

The results of the calculation are shown in figure 10, while the constants used are given in the following table:

	D		$\sigma$		$r_0$	
	kJ/mole	kcal/mole	cm <sup>-1</sup>	Å <sup>-1</sup>	cm	Å
Iron - iron	40.2	9.6	1.389×10 <sup>8</sup>	1.389	1.42×10 <sup>-8</sup>	1.42
Iron - hydrogen	3.39	0.81	4.000×10 <sup>8</sup>	4.000	Variable	Variable

## REFERENCES

1. Elsea, A. R.; and Fletcher, E. E.: Hydrogen-Induced, Delayed, Brittle Failures of High-Strength Steels. DMIC Rep. 196, Battelle Memorial Inst. (AD-601116), Jan. 20, 1964.
2. Johnson, E. W.; and Hill, M. L.: The Diffusivity of Hydrogen in Alpha Iron. Trans. AIME, vol. 218, no. 6, Dec. 1960, pp. 1104-1112.
3. Fletcher, E. E.; and Elsea, A. R.: Hydrogen Movement in Steel - Entry, Diffusion, and Elimination. DMIC Rep. 219, Battelle Memorial Inst. (AD-474578), June 30, 1965.
4. Hill, M. L.; and Johnson, E. W.: The Solubility of Hydrogen in Alpha Iron. Trans. AIME, vol. 221, no. 3, June 1961, pp. 622-629.
5. Coe, F. R.; and Moreton, J.: Diffusion of Hydrogen in Low-Alloy Steel. J. Iron Steel Inst., vol. 204, pt. 4, Apr. 1966, pp. 366-370.
6. Sturges, C. M.; and Miodownik, A. P.: The Interaction of Hydrogen and Dislocations in Iron. Acta Met., vol. 17, no. 9, Sept. 1969, pp. 1197-1207.
7. Wahlin, H. B.; and Mack, D. J.: The Escape of Hydrogen from Iron. Acta Met., vol. 7, no. 10, Oct. 1959, pp. 687-689.
8. Ono, Kanji; and Rosales, Louis A.: On the Anomalous Behavior of Hydrogen in Iron at Lower Temperatures. Trans. AIME, vol. 242, no. 2, Feb. 1968, pp. 244-248.
9. Hill, M. L.; and Johnson, E. W.: Hydrogen in Cold Worked Iron-Carbon Alloys and the Mechanism of Hydrogen Embrittlement. Trans. AIME, vol. 215, no. 4, Aug. 1959, pp. 717-725.
10. Andrew, J. H.; and Lee, H.: Internal Stresses and the Formation of Hairline Cracks in Steel. Symposium on Internal Stresses in Metals and Alloys. Institute of Metals, London, 1947, p. 265.
11. Smith, Donald P.: Hydrogen in Metals. Univ. Chicago Press, 1948.
12. Hill, M. L.: The Behavior of Hydrogen in Iron and Steel. Hydrogen Embrittlement in Metal Finishing. Harold J. Read, ed., Reinhold Publ. Corp., 1961, pp. 46-80.
13. Ham, W. R.; and Rast, W. L.: A Study of the  $A_0$  point of Iron by Diffusion of Hydrogen. Trans. ASM, vol. 26, no. 3, Sept. 1938, pp. 885-902.
14. Keeler, J. H.; and Davis, H. M.: Density and Hydrogen Occlusion of Some Ferrous Metals. Trans. AIME, vol. 197, 1953, pp. 44-48.

15. Evans, G. M.; and Rollason, E. C.: Influence of Non-Metallic Inclusions on the Apparent Diffusion of Hydrogen in Ferrous Materials. *J. Iron Steel Inst.*, vol. 207, pt. 11, Nov. 1969, pp. 1484-1490.
16. Chang, P. L.; and Bennett, W. D. G.: Diffusion of Hydrogen in Iron and Iron Alloys at Elevated Temperatures. *J. Iron Steel Inst.*, vol. 170, pt. 3, Mar. 1952, pp. 205-213.
17. Oriani, R. A.: Hydrogen in Metals. Proceedings of Conference on Fundamental Aspects of Stress Corrosion Cracking. Nat. Assoc. Corrosion Eng., 1969, p. 32.
18. Johnson, R. A.; Dienes, G. J.; and Damask, A. C.: Calculations of the Energy and Migration Characteristics of Carbon and Nitrogen in  $\alpha$ -Iron and Vanadium. *Acta Met.*, vol. 12, no. 11, Nov. 1964, pp. 1215-1224.
19. Girifalco, L. A.; and Weizer, V. G.: Application of the Morse Potential Function to Cubic Metals. *Phys. Rev.*, vol. 114, no. 3, May 1, 1959, pp. 687-690.
20. Pauling, Linus C.: *The Nature of the Chemical Bond*. Third ed. Cornell Univ. Press, 1960.
21. Smialowski, Michal: *Hydrogen in Steel*. Addison-Wesley Publ. Co., 1962.
22. Fletcher, E. R.; and Elsea, A. R.: The Effects of High-Pressure, High-Temperature Hydrogen on Steel. DMIC Rep. 202, Battelle Memorial Inst. (AD-601389), Mar. 26, 1964, p. 16.
23. Gibala, R.: Internal Friction in Hydrogen-Charged Iron. *Trans. AIME*, vol. 239, no. 10, Oct. 1967, pp. 1574-1585.
24. Weiner, L. C.; and Gensamer, M.: The Effects of Aging and Straining on the Internal Friction of Hydrogen Charged 1020 Steel at Low Temperatures. *Acta Met.*, vol. 5, no. 12, Dec. 1957, pp. 692-694.
25. Heller, W. R.: Quantum Effects in Diffusion: Internal Friction Due to Hydrogen and Deuterium Dissolved in  $\alpha$ -Iron. *Acta Met.*, vol. 9, no. 6, June 1961, pp. 600-613.
26. Maringer, R. E.; Swetnam, E. B.; Marsh, L. L.; and Manning, G. K.: Study of Hydrogen Embrittlement of Iron by Internal-Friction Methods. NACA TN 4328, 1958.
27. Lord, A. E., Jr.: Diffusion of Hydrogen in  $\alpha$ -Iron at About 120° K. *Acta Met.*, vol. 15, no. 7, July 1967, pp. 1241-1244.

28. Frank, Robert C.; Swets, Don E.; and Fry, David L.: Mass Spectrometer Measurements of the Diffusion Coefficient of Hydrogen in Steel in the Temperature Range of 25<sup>o</sup>-90<sup>o</sup> C. *J. Appl. Phys.*, vol. 29, no. 6, June 1958, pp. 892-898.
29. Hobson, J. D.: The Diffusion of Hydrogen in Steel at Temperatures of -78<sup>o</sup> to 200<sup>o</sup> C. *J. Iron Steel Inst.*, vol. 189, pt. 4, Aug. 1958, pp. 315-321.
30. Frank, Robert C.; Lee, Robert W.; and Williams, Robert L.: Ratio of the Diffusion Coefficients for the Diffusion of Hydrogen and Deuterium in Steel. *J. Appl. Phys.*, vol. 29, no. 6, June 1958, pp. 898-900.
31. Stross, T. M.; and Tompkins, F. C.: The Diffusion Coefficient of Hydrogen in Iron. *J. Chem. Soc., Pt. 1*, 1956, pp. 230-234.
32. Choi, Jei Y.: Diffusion of Hydrogen in Iron. *Met. Trans.*, vol. 1, no. 4, Apr. 1970, pp. 911-919.
33. Eschbach, H. L.; Gross, F.; and Schullien, S.: Permeability Measurements with Gaseous Hydrogen for Various Steels. *Vacuum*, vol. 13, no. 12, 1963, pp. 543-547.
34. Gonzales, O. D.: The Measurement of Hydrogen Permeation in Alpha Iron: An Analysis of the Experiments. *Trans. AIME*, vol. 245, no. 4, Apr. 1969, pp. 607-612.
35. Geller, Werner; and Sun, Tak-Ho: Influence of Alloy Additions on Hydrogen Diffusion in Iron and Contribution to the Iron-Hydrogen System. *Arch. Eisenhüttenw.*, vol. 21, no. 11/12, Nov./Dec. 1950, pp. 423-430.
36. Borelius, G.; and Lindblom, S.: Passage of Hydrogen Through Metals. *Ann. d. Physik*, vol. 82, 1927, p. 201.
37. Sykes, C.; Burton, H. H.; and Gegg, C.: Hydrogen in Steel Manufacture. *J. Iron Steel Inst.*, vol. 156, pt. 2, June 1947, pp. 155-180.
38. Eichenauer, W.; Kunzig, H.; and Pebler, A.: Diffusion and Solubility of Hydrogen in  $\alpha$ -Iron and Silver. *Zeit. Metallk.*, vol. 49, 1958, p. 220.
39. Carmichael, D. C.; Hornaday, J. R.; Morris, A. E.; and Parlee, N. A.: The Absorption and Effusion of Hydrogen in Alpha Iron. *Trans. AIME*, vol. 218, no. 5, Oct. 1960, pp. 826-832.
40. Barrer, R. M.: Aspects of Gas-Metal Equilibrium, Interstitial Solution and Diffusion. *Discussions Faraday Soc.*, No. 4, 1948, pp. 68-81.
41. Hill, M. L.; and Johnson, E. W.: Hydrogen in Cold Worked Iron-Carbon Alloys and the Mechanism for Hydrogen Embrittlement. *Trans. AIME*, vol. 215, no. 4, Aug. 1959, pp. 717-725.

TABLE I. - VALUES OF PARAMETERS USED TO CALCULATE THE HEATS OF SOLUTION  
IN THE HIGH- AND LOW-TEMPERATURE REGIONS

Temperature region	Experimental activation energy for permeation, $Q_p$		Source reference	Experimental activation energy for diffusion, $Q_d$		Calculated heat of solution, $Q_s$	
	kJ/mole	kcal/mole		kJ/mole (a)	kcal/mole (a)	kJ/mole	kcal/mole
High	38.6	9.2	13	10.5	2.5	28.1	6.7
	36.9	8.8	16	10.5	2.5	26.4	6.3
Low	76.7	18.3	13	29.3	7	47.4	11.3
	74.2	17.7	16	29.3	7	44.8	10.7

<sup>a</sup>Average values from the literature (see fig. 13).